ISSN 1674-1056
http://cpb.iphy.ac.cn
http://iopscience.iop.org/cpb
中国物理 B
Chinese Physics
中国物理
Chinese Physics B

Attractors with controllable basin sizes from cooperation of contracting and expanding dynamics in pulse-coupled oscillators

Hai-Lin Zou(邹海林), Zi-Chen Deng(邓子辰)

Citation: Chin. Phys. B . 2019, 28(1): 010502. **doi:** 10.1088/1674-1056/28/1/010502
Journal homepage: http://cpb.iphy.ac.cn; http://iopscience.iop.org/cpb

What follows is a list of articles you may be interested in

Primary resonance of fractional-order Duffing-van der Pol oscillator by harmonic balance method

Sujuan Li(李素娟), Jiangchuan Niu(牛江川), Xianghong Li(李向红)

Chin. Phys. B . 2018, 27(12): 120502. **doi:** 10.1088/1674-1056/27/12/120502

Bursting oscillations as well as the bifurcation mechanism in a non-smooth chaotic geomagnetic field model

Ran Zhang(张冉), Miao Peng(彭淼), Zhengdi Zhang(张正娣), Qinsheng Bi(毕勤胜)

Chin. Phys. B . 2018, 27(11): 110501. **doi:** 10.1088/1674-1056/27/11/110501

A new four-dimensional hyperjerk system with stable equilibrium point, circuit implementation, and its synchronization by using an adaptive integrator backstepping control

J P Singh, V T Pham, T Hayat, S Jafari, F E Alsaadi, B K Roy

Chin. Phys. B . 2018, 27(10): 100501. **doi:** 10.1088/1674-1056/27/10/100501

Nonlinear suboptimal tracking control of spacecraft approaching a tumbling target

Zhan-Peng Xu(许展鹏), Xiao-Qian Chen(陈小前), Yi-Yong Huang(黄奕勇), Yu-Zhu Bai(白玉铸), Wen Yao(姚雯)

Chin. Phys. B . 2018, 27(9): 090501. **doi:** 10.1088/1674-1056/27/9/090501

Conservation laws for Birkhoffian systems of Herglotz type

Yi Zhang(张毅), Xue Tian(田雪)

Chin. Phys. B . 2018, 27(9): 090502. **doi:** 10.1088/1674-1056/27/9/090502

Attractors with controllable basin sizes from cooperation of contracting and expanding dynamics in pulse-coupled oscillators*

Hai-Lin Zou(邹海林)† and Zi-Chen Deng(邓子辰)

School of Mechanics, Civil Engineering and Architecture, Northwestern Polytechnical University, Xi'an 710072, *China*

(Received 4 September 2018; revised manuscript received 22 October 2018; published online 25 December 2018)

Unstable attractors are a novel type of attractor with local unstable dynamics, but with positive measures of basins. Here, we introduce local contracting dynamics by slightly modifying the function which mediates the interactions among the oscillators. Thus, the property of unstable attractors can be controlled through the cooperation of expanding and contracting dynamics. We demonstrate that one certain type of unstable attractor is successfully controlled through this simple modification. Specifically, the staying time for unstable attractors can be prolonged, and we can even turn the unstable attractors into stable attractors with predictable basin sizes. As an application, we demonstrate how to realize the switching dynamics that is only sensitive to the finite size perturbations.

Keywords: unstable attractors, switching dynamics, pulse-coupled oscillators

PACS: 05.45.–a, 05.45.Xt, 87.19.lj **DOI:** 10.1088/1674-1056/28/1/010502

1. Introduction

Attractors in nonlinear dynamical systems are used to represent long term dynamics, which are the most essential feature of nonlinear dynamical systems.[1,2] The set of initial conditions that can lead to an attractor is defined as its basin of attraction. The separations among basins are the basin boundaries. For a conventional stable attractor, the attractor is enclosed in its basin. We thus can quantify the strength of an attractor by the basin size which is the closest distance between the attractor and its basin boundaries. Typically, the basin boundaries are the stable manifold of saddle points. However, for hidden attractors, their corresponding basins do not intersect with small neighborhoods of any equilibrium points.[3–6]

Another interesting dynamic is meta-stable states, the system can stay near the vicinity of the meta-stable states for a relatively long time. Meta-stable dynamics is usually due to the appearance of saddles, and the switching dynamics among meta-stable states is regarded as useful for information processing.[7] Usually attractors and meta-stable states are two quite different dynamical states. However, unstable attractors are saddles but with positive measures of basins.[8–10] Hence this type of attractor is defined in the sense of Milnor attractors.[11] For these attractors, almost all nearby points within a neighborhood will leave the attractors, leading to a zero basin size. But the remote region in phase space could collapse into the stable manifold of saddles.[12] Another interesting type of attractor, i.e., partially unstable attractors, with both stable and unstable points can also appear in pulse-coupled oscillators under periodic forcing.[13]

Unstable attractors are observed in pulse-coupled oscillators with delays, where the delays account for the transmission time of the pulses.[14–19] Such models can be used to study various natural phenomena, such as neural dynamics where pulses correspond to the generations of spikes, and synchronization of fireflies where pulses are the flashes. The interactions among oscillators are mediated by the pulses. The generation and arrival of pulses are then important events. We can introduce symbolic events based on the related events, which are useful for understanding the unstable attractors.[20,21]

One typically application of these attractors is used to generate switching dynamics among these states.[7,22–26] The switching dynamics built upon unstable attractors is sensitive to infinitesimal perturbations. Thus any small noise can induce switching phenomena. One desirable feature is that switching dynamics is only sensitive to finite size perturbations. Thus how to explicitly manipulate these unstable attractors is interesting and important to the applications built upon these novel saddles. In this paper, we present a method to control unstable attractors towards attractors with controllable basin sizes. We first identify the local expanding dynamics and then introduce the local contracting dynamics. The basin sizes and staying time can be controlled by the cooperation of expanding and contracting dynamics.

This paper is organized as follows. In Section 2, the model of pulse-coupled oscillators is described, and also the evolution rate for the local expanding dynamics is derived. In Section 3, we introduce the contracting dynamics, investigate the local dynamic behavior, and derive the condition of the appearance of contracting dynamics. In Section 4, we investigate the staying time and attractors with controllable basin

*Project supported by the National Natural Science Foundation of China (Grant Nos. 11502200 and 91648101) and the Fundamental Research Funds for the Central Universities, China (Grant No. 3102018zy012).

†Corresponding author. E-mail: zouhailin@nwpu.edu.cn

© 2019 Chinese Physical Society and IOP Publishing Ltd

sizes, and we realize the switching dynamics that are only sensitive to perturbations larger than the basin sizes. Finally, the conclusion and discussion are presented.

2. Unstable attractors with local expanding dynamics

2.1. Networks of pulse-coupled Millro–Strogatz oscillators

Here we consider the pulse-coupled Millro–Stragatze oscillators,[14] where the state for an oscillator i is described by a phase-like variable ϕ_i. The free dynamics is given by

$$\mathrm{d}\phi_i/\mathrm{d}t = 1. \tag{1}$$

When the oscillator i reaches the threshold 1, the state is reset to zero. During this process, the oscillator i fires, and a pulse is generated and sent to oscillators with incoming links from i. After a delay time τ, the arrival of the pulse can induce a phase jump for the oscillators who have incoming links from oscillator i. For example, the arrival of the pulse from oscillator i could induce a phase jump for oscillator j according to

$$\phi_j(t^+) = \min[1, U_b^{-1}(U_b(\phi_j(t)) + \varepsilon_{ji})], \tag{2}$$

where function $U_b(x)$ is given by

$$U_b(x) = \frac{1}{b}\ln[1 + (\exp(b) - 1)x]. \tag{3}$$

Here b is a positive parameter (fixed at 3 throughout the paper), and ε_{ji} denotes the coupling strength from oscillator i to j. The ε_{ji} is normalized according to the number of incoming links for oscillator i, i.e., $\varepsilon_{ji} = \varepsilon/k_i$, where k_i is the number of incoming links for oscillator i. Here we consider the globally coupled oscillators without self-links. Thus,

$$\varepsilon_{ji} = \varepsilon/(N-1) \tag{4}$$

for networks with N oscillators. When the couplings are positive with $\varepsilon_{ij} > 0$, the couplings are excitatory. The arrival of pulses makes the states of corresponding oscillators closer to the threshold. Unstable attractors typically arise for small τ and ε, such as $0 < \tau < 0.3$ and $0 < \varepsilon < 0.3$.[20] Here we also focus on the unstable attractors occurring in this region. The parameter N is the number of oscillators, which highly affects the dimension of the system. In this paper, we choose $N = 4$ and $N = 15$ to represent relatively low- and high-dimensional systems, respectively.

2.2. Source of local unstable dynamics revealed by symbolic events

For the globally coupled oscillators with excitatory couplings, i.e., with positive ε, there exist unstable attractors. Here we can choose one oscillator such as oscillator 1 as the reference. When this reference oscillator fires, the states of the whole system are recorded. In this way, we actually construct a return map, i.e., the Poincaré map, where the time is represented by the n-th reset of the reference oscillator. In this return map, the unstable attractors are of period one.

We exploit the event properties to reveal the unstable dynamics, which are useful to explore the unstable source here. When the state of an oscillator i reaches the threshold 1, it fires and its state is immediately reset to zero. During this process, a pulse is generated and sent out. After delay time τ, the pulse will be received by oscillators with incoming links from oscillator i. The specific notations are first introduced. The firing of oscillator i is denoted by S_i, and the arrival of pulses from oscillator j is denoted by R_j. The events at different times are separated by "–". For example, the event structure for the unstable attractor shown in Fig. 1(a) is given by

$$R_1S_4 - R_4 - S_2S_3 - R_2R_3S_1, \tag{5}$$

where two oscillators 2 and 3 reach the threshold simultaneously during free evolution. These firings are called active firings, while other firings are directly due to the arrival of pulses, and then called passive firings. The two oscillators 2 and 3 receive the same amount of pules at the arrival of pulses, and hence can keep the simultaneous firing events. The simultaneous active firing is responsible for the unstable nature of the unstable attractors.[20] Just after the firing of oscillators 2 and 3 (i.e., S_2S_3), they will receive pulses from themselves (i.e., $R_2R_3S_1$) after delay time τ. Thus just before the arrival of these pulses, the state for oscillators 2 and 3 is τ.

Figure 1(b) demonstrates that the split of simultaneous active firing, such as S_2S_3 here, is responsible for the local unstable dynamics. The unstable attractor is denoted by "+" in the (ϕ_2, ϕ_3) subspace. We can see that the unstable attractor displays the saddle property. The non-identical perturbations δ_2 and δ_3 split the simultaneous firing and make the system leave the unstable attractor. The system follows the unstable local directions, similar to the unstable manifold of a saddle. If the perturbations δ_2 and δ_3 are the same, then the system can actually jump back to the original unstable attractor, similar to the stable manifold.

In this paper, we mainly focus on the unstable attractors of event structures similar to Eq. (5) where only two oscillators are simultaneously firing. To control the cases with a large number of simultaneously firing oscillators is challenging, mainly due to the complex jump in phase state due to the split of simultaneously firing.[8] Thus at the first step, we focus on the control of the unstable attractors with only two simultaneously firing oscillators, which will shed light on solving the problem of controlling all unstable attractors.

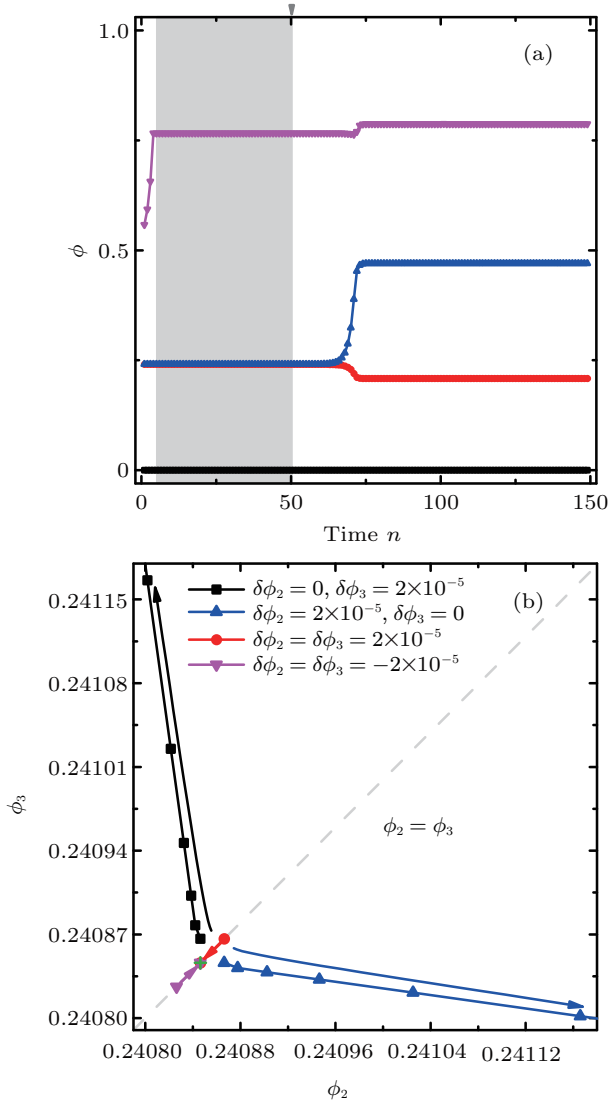


Fig. 1. (a) An unstable attractor highlighted in gray is located with a randomly selected initial condition in four globally coupled oscillators. The four curves represent the states of the four oscillators respectively, which are recorded just after the n-th reset of the reference oscillator 1. Upon the perturbations introduced at the arrow position, the system will leave the attractor, indicating its unstable nature. (b) The dynamics in the (ϕ_2, ϕ_3) is shown, the existence of the two simultaneous active firing oscillators 2 and 3 is responsible for the unstable dynamics. The "+" denotes the unstable attractor. The different perturbations on oscillators 2 and 3 can split the simultaneous firing and make the system leave the unstable attractor (similar to the unstable manifold of a saddle). While the perturbations with $\delta\phi_2 = \delta\phi_3$ cannot split the simultaneous firings and the system can lead to the unstable attractor (similar to the stable manifold). The parameters are chosen as $N = 4$, $b = 3$, $\varepsilon = 0.15$, and $\tau = 0.2$.

2.3. Evolution rate due to the local expanding dynamics

In the presence of perturbations, the system will leave the unstable attractor. The staying time describes how long the system can stay near the unstable attractor. We analyze in detail the unstable local dynamics for an unstable attractor. In order to control the unstable attractors, we need to control the unstable local dynamics.

We can only focus on the dynamics of multiple active firing oscillators. Here the phases of the active firing oscillators change fast, while the phases of the other passive firing oscillators change slowly. Thus we can focus on the phases of the active firing oscillators when analyzing local dynamics. By exploring the local behaviors, we select the nearby points of an unstable attractor. This can be realized by randomly adding perturbations on each oscillator.

Under the randomly selected perturbations, the simultaneous active firings will be split into multiple single firings at slightly different times. This introduces initial phase differences among the active firing oscillators. We consider two oscillators p and q. The free dynamics cannot change the phase difference here. Thus we only consider the arrival of pulses. Then the phase difference is changed due to the arrival of pulses from oscillators other than p and q, and the pulses from themselves.

Here the unstable attractors are period one attractors, when using one oscillator as the reference, as shown in Fig. 1(a). In this case, all oscillators only fire once during one time period. Thus we quantify the local dynamic by considering the evolution rate of phase difference between two active firing oscillators. Suppose that the initial small phase difference is Δ_0, then the phase difference after one time period is Δ_1. Then the evolution rate is defined as

$$R = \frac{\Delta_1}{\Delta_0}. \tag{6}$$

In the following, we analyze the evolution rate for the unstable attractor by considering the effect of pulses on the phase difference of two active firing oscillators.

2.3.1. The effect of pulses from other non-active firing oscillators

We first consider the pulse from other non-active firing oscillators. Suppose that a pulse with strength ε' arrived at time t. Just before the arrival of the pulse, the phase difference is $\Delta\phi^- = \phi_p - \phi_q$. Then just after the arrival of the pulse, the phase difference becomes

$$\Delta\phi^+ = U_b^{-1}[U_b(\phi_p) + \varepsilon'] - U_b^{-1}[U_b(\phi_q) + \varepsilon'].$$

By plugging $U_b(x)$ and $U_b^{-1}(x)$ into the above equation, we can obtain

$$\Delta\phi^+ = \exp(b\varepsilon')\Delta\phi^-.$$

Thus a pulse with strength ε' can change the rate as $\Delta\phi^+/\Delta\phi^- = \exp(b\varepsilon')$. By considering all other oscillators such as the pulse from oscillator i with strength ε_i, the total change of rate R_o due to other non-active firing oscillators is

$$R_o = \prod_i \exp(b\varepsilon_i).$$

Then for the two active firing oscillators, they receive pulses from all other $N-2$ oscillators, each pulse with strength $\varepsilon/(N-1)$. Then the total rate of change R_o due to the pulses from the other oscillators is

$$R_o = \exp[b\varepsilon((N-2)/(N-1))]. \tag{7}$$

2.3.2. The effect of pulses from active firing oscillators

Then we consider the effects of arrival of pulses from two active firing oscillators themselves. Now let oscillator p fire first, followed by q. Then we consider the effect of a piece of events $S_p - S_q - R_p - R_q$. Just after the firing of q, the states are x and 0 for oscillators p and q, respectively. Then the phase difference is x. We then need to obtain the states just after R_q. For the oscillator q, it undergoes free evolution $\tau - x$, and then receives the pulse from p, and then it undergoes free evolution of x. The state for oscillator q just after the event R_q is

$$\phi_q^{\rm s} = U_b^{-1}[U_b(\tau - x) + \varepsilon'] + x.$$

For oscillator p, it first undergoes free evolution for τ, then it receives a pulse from q after additional time x. The state just before the arrival of the R_q is $\tau + x$. Thus,

$$\phi_p^{\rm s} = U_b^{-1}[U_b(\tau + x) + \varepsilon'].$$

Then the phase difference between oscillators p and q just after the event R_q becomes

$$\phi_p^{\rm s} - \phi_q^{\rm s} = [2\exp(b\varepsilon') - 1]x.$$

Then the change of phase difference due to the arrival of pulses form p and q is defined as $R_{\rm s} = (\phi_p^{\rm s} - \phi_q^{\rm s})/x$, which is

$$R_{\rm s} = [2\exp(b\varepsilon') - 1]. \tag{8}$$

2.3.3. The effect of all pulses

Thus the phase difference between p and q is increased due to the pulses from other non-active firing oscillators (see Eq. (7)) and pulse from themselves (see Eq. (8)). Then during one reset of the reference oscillator, the total rate $R_{\rm T}$ is

$$\begin{aligned} R_{\rm T} &= R_{\rm o} \times R_{\rm s} \\ &= \exp[b\varepsilon((N-2)/(N-1))] \times [2\exp(b\varepsilon') - 1]. \end{aligned} \tag{9}$$

Under the present choice of $U_b(x)$, the arrival of pulses can increase the phase difference of the active firing oscillators. Thus the effect of arrival of pulses is expanding.

3. Introducing contracting dynamics

The effects of pulses are expanding for the active firing oscillators under the current function, in the sense that the phase difference for any two active firing oscillators increases. In order to manipulate or control these unstable attractors, an intuitive way is to introduce the contracting dynamics so that the arrival of certain pulses could decrease the phase differences among the active firing oscillators. Thus we slightly modified the function $U_b(x)$ in Eq. (3), which mediates the pulse interactions among the oscillators.

3.1. The slightly modified function

Intuitively, the introduction of contracting dynamics is possible. For example, we can make the function in Eq. (3) behave close to a horizontal line in a certain interval where a pulse is received. Then the phase response of two oscillators at slightly different states can actually become close to each other, and hence the corresponding phase difference decreases. Then we consider which interval we should choose to modify the function. To this end, we consider the state of the active firing oscillators. We modify the effect of pulses from these active firing oscillators. Just before the arrival of these pulses, the states of the active firing oscillators are near τ. This is typically true when τ is not relatively large.[21]

Thus we slightly modify the function in the interval $[\tau - c, \tau + c]$, where c determines the width of the interval and should be small enough. In this paper, we choose $c = 10^{-4}$ and $c = 10^{-5}$ as two typical small values. For simplicity, we still use the same form of function $U_b(x)$ but with different parameters within this interval. To be distinguishable, the parameter is denoted by B. The function in the interval [0,1] is continuous. We will show later that c is directly related to the controlled basin sizes.

Thus the new function $\tilde{U}(x)$ has two parameters b and B, which is given by

$$\tilde{U}(x) = \begin{cases} (y_2 - y_1)U_B\left(\dfrac{x - x_1}{2c}\right) + y_1, & x_1 \leqslant x \leqslant x_2, \\ \dfrac{1}{b}\ln[1 + (\exp(b) - 1)x], & \text{otherwise}, \end{cases} \tag{10}$$

where $x_1 = \tau - c, x_2 = \tau + c$, $y_1 = U_b(x_1)$, and $y_2 = U_b(x_2)$.

When $|B|$ is sufficiently large, the above function in the small interval $[x_1, x_2]$ becomes horizontal. Then upon the arrival of a pulse, the states of the oscillators within this interval can become closer to each other. Hence contracting dynamics occurs. Other forms of functions which behave horizontally in the interval $[x_1, x_2]$ can also introduce contracting dynamics and hence can also work. Figure 2 shows an example of the modified function.

3.2. The contracting dynamics induced by the modified function

Here we first investigate how to choose the parameter c which determines the interval for the modified function. The value of c should be small enough, such that global dynamics of the system is not much disturbed. In the following, we analyze the detailed condition for c, with the consideration of simplification on the analysis.

Upon the arrival of a pulse from one active firing oscillator, the state of one of the other oscillators is ϕ, satisfying $\tau - c < \phi < \tau + c$. Then suppose that the arrived pulse is of strength ε'. According to the response process, we need

to consider the value $y = \tilde{U}(\phi) + \varepsilon'$. The value of y determines which part of the inverse function we should use. If $y > U_b(\tau + c)$, we should apply the inverse function of $U_b(y)$. Otherwise, we should apply the inverse function $\tilde{U}(y)$. When c is much smaller than ε', the first case is always satisfied. This process is shown in Fig. 2.

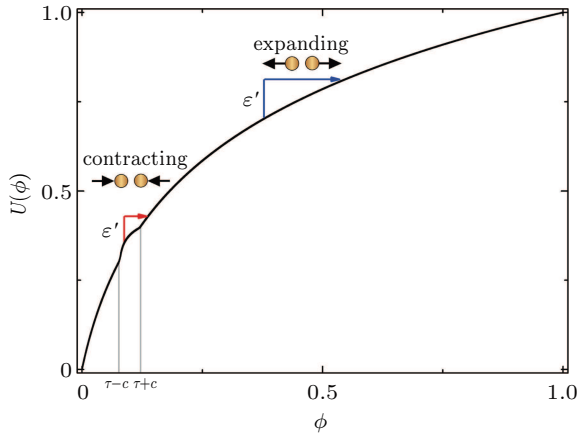


Fig. 2. The function $\tilde{U}(x)$ by modifying the function in the interval $[\tau - c, \tau + c]$. The arrival of a pulse with strength ε' in this interval can induce contracting dynamics in the sense that the phase difference of two active firing oscillators decreases, while other pulses can induce expanding dynamics.

Then the arrival of a pulse with strength ε' for an oscillator with state ϕ could induce a phase change as

$$\phi^+ = U_b^{-1}\left[(y_2 - y_1)U_B\left(\frac{\phi - x_1}{2c}\right) + y_1 + \varepsilon'\right].$$

The right-hand side of the above equation is frequently applied later, and is defined as a new function

$$\begin{aligned} &F(\phi, \varepsilon', b, B) \\ &= U_b^{-1}\left[(y_2 - y_1)U_B\left(\frac{\phi - x_1}{2c}\right) + y_1 + \varepsilon'\right]. \end{aligned} \tag{11}$$

We then choose two active firing oscillators, and study their evolution of phase difference under the new function. Here we first consider the effect of pulses from the active firing oscillators on the phase difference. The two oscillators are p and q, and assume that p fires first. Then we encounter a piece of events $S_p - S_q - R_p - R_q$. Just after the event S_q, the states for p and q are x and 0, respectively, with x close to zero. Thus the phase difference between the two oscillators is x. We then calculate the phase difference just after the event R_q. For oscillator q, it receive a pulse from p (i.e., event R_p) with phase $\tau - x$. After x time, the pulse from itself is received (i.e., event R_q), its phase will increase further by x due to the free evolution Eq. (1). Then the phase of oscillator q is

$$\phi_q = F(\tau - x, \varepsilon', b, B) + x.$$

For oscillator p, the phase at event R_q can be obtain similarly, which is

$$\phi_p = F(\tau + x, \varepsilon', b, B).$$

Then we find that the phase difference is changed from x to $\phi_p - \phi_q$. We obtain the rate of phase change, $\tilde{R}_s = (\phi_p - \phi_q)/x$, due to the arrival of the pulses from themselves, which is

$$\tilde{R}_s = \frac{F(\tau + x, \varepsilon', b, B) - F(\tau - x, \varepsilon', b, B)}{x} - 1. \tag{12}$$

Here x is the initial small phase difference for the two active firing oscillators. The $\tilde{R}_s$ depends on the initial phase difference x. We find that this function is monotonous on x. The minimum value is obtained when x is near zero. Thus,

$$\tilde{R}_s^{\min} = -1 + 2\frac{\mathrm{d}F(\tau + x, \varepsilon', b, B)}{\mathrm{d}x}\Big|_{x=0}. \tag{13}$$

By using

$$\frac{\mathrm{d}F(\tau + x, \varepsilon', b, B)}{\mathrm{d}x}\Big|_{x=0} = 2\mathrm{e}^{b\varepsilon'}\frac{\mathrm{e}^B - 1}{B(\mathrm{e}^B + 1)},$$

equation (13) becomes

$$\tilde{R}_s^{\min} = 4\mathrm{e}^{b\varepsilon'}\frac{\mathrm{e}^B - 1}{B(\mathrm{e}^B + 1)} - 1. \tag{14}$$

The $\tilde{R}_s$ quantifies the change of phase difference due to the pulses from themselves. If it becomes less than 1, then the effect becomes contracting.

4. Cooperation of expanding and contracting dynamics

Then we consider the total effect of pulses on the evolution rate during one time period. Again, the contributions can be classified into two parts. One contribution comes from the active firing oscillators as described in Eq. (12). The other contribution comes from the non-active firing oscillators. As the active firing oscillators receive the pulses at the state outside the interval $[\tau - c, \tau + c]$, then the total effect of these pulses is the same as R_o in Eq. (7). Then the total rate $\tilde{R}_T$ after one time period is

$$\tilde{R}_T = \tilde{R}_s \times R_o. \tag{15}$$

When the initial phase difference is close to zero, the evolution rate is minimal given by

$$\tilde{R}_T^{\min} = \tilde{R}_s^{\min} \times R_o. \tag{16}$$

The critical condition is $\tilde{R}_T = 1$, which is shown in Fig. 3. The value of $\tilde{R}_T$ is symmetrical with respect to B. In the middle region II, the value of $\tilde{R}_T$ is always larger than 1, indicating expanding behaviors. Then if we increase $|B|$, $\tilde{R}_T$ decreases. In the case $\tilde{R}_T < 1$, the phase difference actually decreases after perturbations, and contracting dynamics dominates. In this case, the unstable attractor becomes a stable attractor, we analyze the basin size in the following subsection. The critical value of B is determined by $\tilde{R}_T^{\min} = 1$.

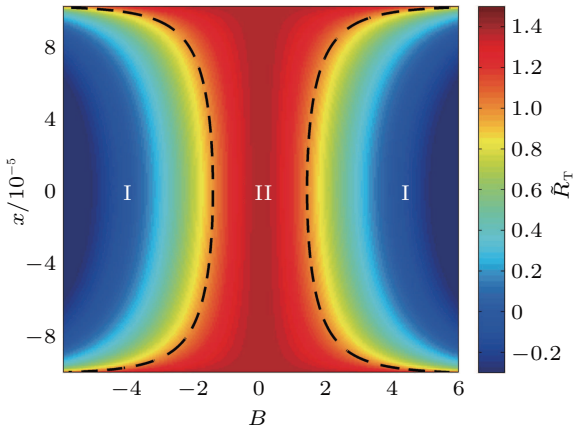


Fig. 3. Regions I and II are the stable and unstable regions, respectively, which are separated by dashed lines obtained according to the critical condition $\tilde{R}_T = 1$. The parameters are $N = 15$, $b = 3$, $\varepsilon = 0.1$, $\tau = 0.1$, and $c = 10^{-5}$.

4.1. Controlled basin size

In the case that $\tilde{R}_T < 1$, the unstable attractor becomes a stable attractor. Here we investigate the controlled basin size d. As shown in Fig. 3, region I corresponds to the case with $\tilde{R}_T < 1$. The range of x in region I determines the basin size. Thus the basin size grows with the increase in $|B|$, and approaches c. Thus for large $|B|$, $d \approx c$. This can also be understood intuitively as follows. If $d > c$, the phase for an oscillator could be $\tau + d$ or $\tau - d$. Note that the chosen modified interval is $[\tau - c, \tau + c]$. Then the arrival of pulses from the active firing oscillators falls out of this region.

Then we estimate the basin sizes. Here we study the dynamics in the return map with one oscillator as reference. Just after the reset of the reference oscillator, we add perturbations. The order of events sequence also matters. In the above analysis, we assume that the pulses from the active firing oscillators are received first. In the case that they are received last, the phase difference between the two active firing oscillators increases first due to the arrival of pulses from the other oscillators. Thus the initial phase difference x is increased to $x \times R_o$ which should be smaller than $x\exp(\varepsilon b)$. Thus we can approximate the basin size as

$$\frac{c}{\exp(\varepsilon b)} < d < c, \tag{17}$$

where $|B|$ is much larger than its critical value.

We verify the above results by using $N = 4$ globally coupled oscillators with fixed parameters $b = 3$ and $\varepsilon = 0.15$. Figure 4(a) shows the controlled basin sizes for the unstable attractors with the parameter B and $\tau = 0.18$. For each B, 100 randomly chosen initial conditions are used to locate the attractors. Here the critical value of B_{cr} is 2.07. When B is smaller than B_{cr}, the original unstable attractors are still unstable with a basin size of zero. When B becomes larger than B_{cr}, the basin sizes become larger than zero and approaches $c = 10^{-5}$. In this case, the basin sizes will finally fall within the predicted values of Eq. (17).

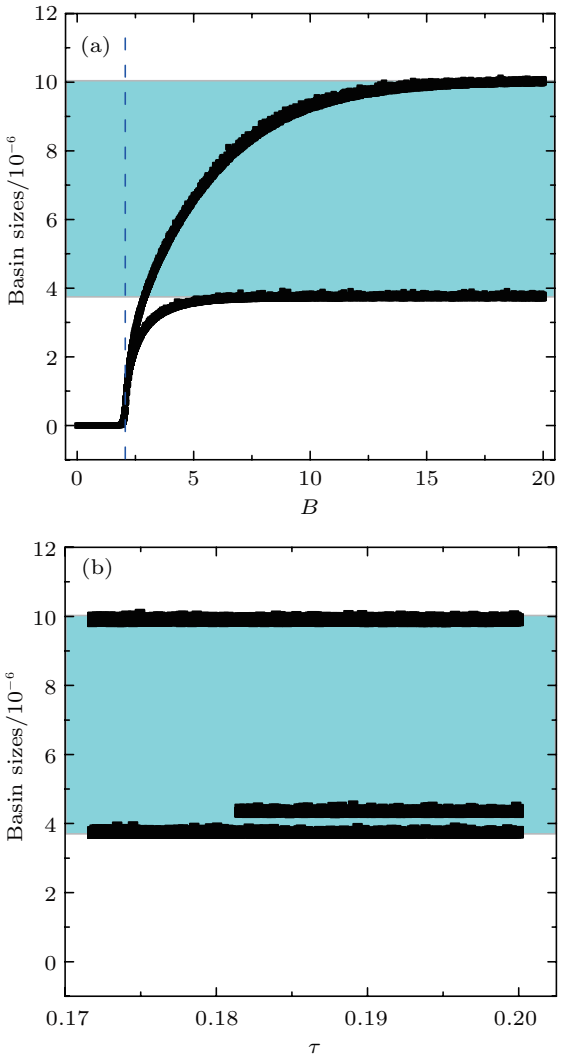


Fig. 4. The controlled basin sizes for $N = 4$ globally coupled oscillators with fixed parameters $b = 3$ and $c = 10^{-5}$. (a) The dependence of the basin sizes on the parameter B with fixed parameters $\varepsilon = 0.15$ and $\tau = 0.18$, where the critical value of B is 2.07 indicated by the dashed vertical line. (b) The dependence of the basin sizes on the parameter τ with fixed parameters $\varepsilon = 0.15$ and $B = 15.0$. Here the shaped region denotes the basin size predicted by Eq. (17) when B is much larger than the critical value.

Furthermore, we choose a larger value of $B = 15$ and let τ be a variable. Then we uniformly choose 1000 values of τ from the interval $[0.17, 0.21]$, where unstable attractors prevail. For each τ, 100 randomly chosen initial conditions are used to locate the attractors. If the attractors are of a structure similar to Eq. (5), we then obtain the basin size. In Fig. 4(b), the dependence of the basin sizes on the parameter τ is shown. Again, we can see that the basin sizes are well predicted by Eq. (17). As long as the value of B is much larger than the critical value, the contracting dynamics dominates, and hence the controlled basin sizes can be predictable. Additionally, the method does not depend on the system parameters as demonstrated in Fig. 4(b).

Then we show a detailed example in Fig. 5 for a relatively higher system with $N = 15$ globally coupled oscillators. The parameters are chosen as $b = 3$, $\varepsilon = 0.2$, $\tau = 0.1$, $B = 5$, and $c = 10^{-4}$. Under the current parameter setting, we

can locate an attractor with oscillators 6 and 7 as the simultaneous active firing oscillators, which should be an unstable attractor without control. Then we change the phase of oscillators 6 and 7 by $\phi_6 = \phi_6 + \Delta\phi_6$ and $\phi_7 = \phi_7 + \Delta\phi_7$. We can see that the system is stable to small perturbations, indicated by the region enclosed by the dashed lines. The dashed line is predicted by $\phi_6 - \phi_7 = x_{\rm cr}$ and $\phi_6 - \phi_7 = -x_{\rm cr}$, where $x_{\rm cr} = c/\exp(0.2 \times 3.0) = 5.5 \times 10^{-5}$.

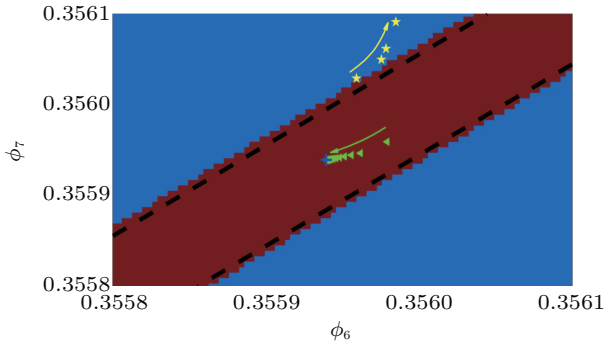


Fig. 5. An original unstable attractor with oscillators 6 and 7 as the active firing oscillators is successfully controlled to be a stable attractor marked by "+". The red region denotes its basin, where the basin size is correctly predicted as shown by the dashed line. The nearby point within the basin leads to the stable attractor as shown in green ◀, while the nearby point outside the basin leaves the stable attractor as shown in yellow ⋆. The parameters are chosen as $N = 15$, $b = 3$, $\varepsilon = 0.2$, $B = 5$, and $c = 10^{-4}$.

4.2. The leaving process and the staying time

Here we first consider the case with $\tilde{R}_{\rm T}^{\rm min} > 1$. In this case, the local dynamics is unstable. The appearance of contracting dynamics can make $\tilde{R}_{\rm T}$ approach 1, which can increase the staying time. Thus we can use B to control the staying time. As an example, we choose the global network with $N = 15$. For $B > 0$, the critical value $B_{\rm cr} = 1.4218$ for $\varepsilon = 0.1$, $\tau = 0.1$, and $b = 3$. Figures 6(a)–6(c) show the staying time for an unstable attractor with different parameter B, each with the same initial condition. We can see that the staying time increases when B approaching $B_{\rm cr}$.

We then investigate in detail the leaving process. According to Eq. (16), when the phase difference is much smaller than c, the change rate can be approximated by

$$L_1 = \tilde{R}_{\rm T}^{\rm min}. \tag{18}$$

By plugging the parameters associated with Fig. 6(c) into the above equation, i.e., $N = 15, b = 3, \varepsilon = 0.1, c = 10^{-4}$, and $B = 1.39$, we can obtain $L_1 = 1.014$. Then the phase difference is increased, becoming larger than c. The evolution rate becomes close to that given in Eq. (9), which is

$$L_2 = R_{\rm T}. \tag{19}$$

By plugging the parameters associated with Fig. 6(c) into the above equation, i.e., $N = 15, b = 3, \varepsilon = 0.1, c = 10^{-4}$, and $B = 1.39$, we can obtain $L_2 = 1.378$. In Fig. 6(d), the evolution of the phase difference is plotted with time n. We can observe two stages of leaving process.

In the case of $\tilde{R}_{\rm T} < 1$, the unstable attractors become stable with basin size predicted by Eq. (17) for large enough $|B|$. Here the system cannot leave the attractor for small perturbations which fall into the basin. However, large perturbations can bypass the basin size and make the system leave the attractor. In such cases, the leaving process manifests as a single process and is described by Eq. (19).

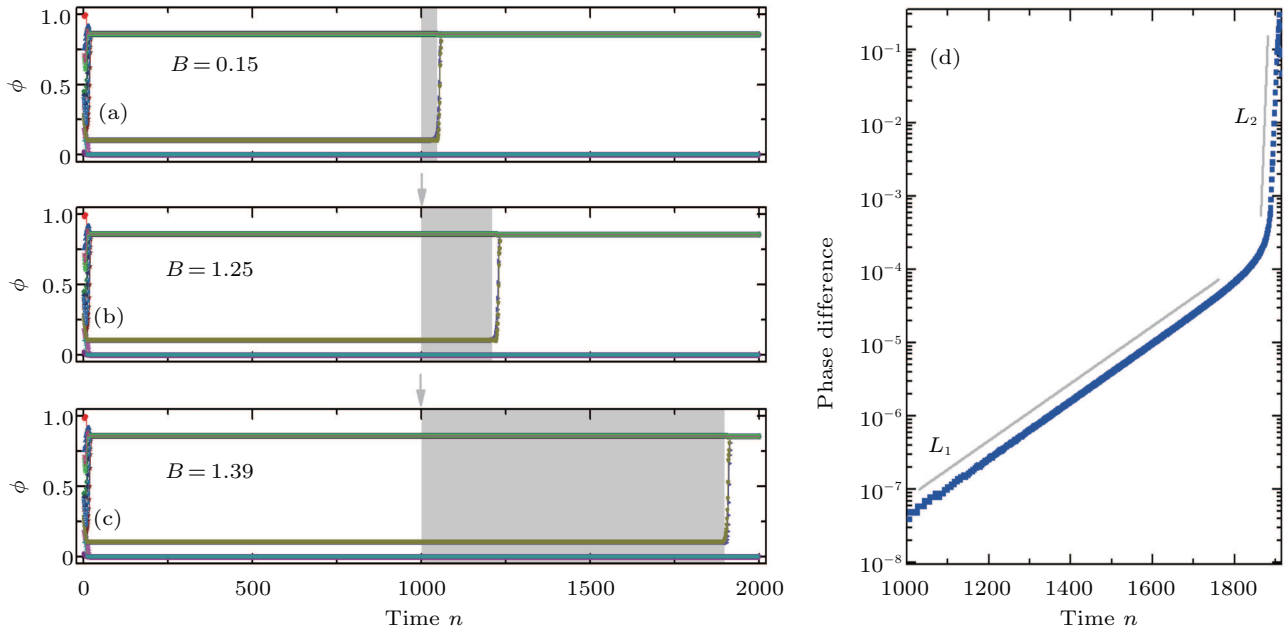


Fig. 6. (a)–(c) The staying time for an unstable attractor is controlled. The staying time (highlighted in gray) becomes longer by decreasing B. (d) For the leaving process in (c), the evolution of phase difference for two active oscillators with time n reveals two processes with two different evolution rates as predicted. The parameters are $N = 15$, $b = 3$, $\varepsilon = 0.1$, $\tau = 0.1$, and $c = 10^{-4}$. The time n denotes the n-th reset of the reference oscillator 1.

4.3. Switching dynamics from attractors with controllable basin size under finite-size perturbations

One typical application of unstable attractors is to generate switching dynamics, which can reflect the input information. The switching among unstable attractors is sensitive to infinitesimally small perturbations. Hence the switching dynamics is not robust to typically unwanted small noise.

Here we show that the controlled attractors with predictable basin sizes can be used to generate switching dynamics that are insensitive to small perturbations. This can be achieved by making the basin sizes larger than the strength of small perturbations. The perturbed trajectories are still within the basin, hence the switching phenomenon cannot occur. However, in the presence of larger perturbations, the system can bypass the controlled small basin size, and generate switching dynamics.

As an example, we consider the system of $N = 15$ oscillators, with $c = 10^{-4}$, $B = -2.0$, $\varepsilon = 0.1$, and $b = 3$. The basin sizes of the controlled unstable attractors are of the order c. We first introduce small random perturbations with the strength $0.1c$ on each oscillator at the three arrow positions. As shown in Fig. 7(a), there is no switching phenomenon under these small perturbations. In order to generate switching dynamics, sufficient strong perturbations should be introduced. Thus we consider the random perturbations with the strength $5c$, such that the system can bypass the controlled interval. As shown in Fig. 7(b), switching dynamics among three metastable states can be observed. This also implies that the three corresponding stable attractors arise from the three controlled unstable attractors. Thus the basin sizes are of the order c. Under the large perturbations, the system can bypass such small basins and generate switching dynamics.

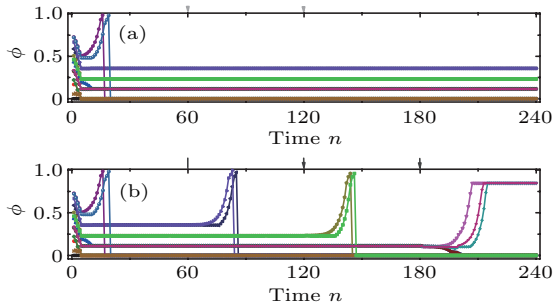


Fig. 7. (a) Controlled unstable attractors with basin sizes of the order c are insensitive to small perturbations such as of the order $0.1c$, which are introduced at the arrow positions. (b) The strong perturbations of the strength $5c$ can induce subsequent switching among different attractors. The parameters are chosen as $N = 15$, $b = 3$, $\varepsilon = 0.1$, $\tau = 0.1$, $B = 2$, and $c = 10^{-4}$.

5. Discussion and conclusion

In summary, we study the control of unstable attractors. We first identify the local expanding dynamics for these attractors. In order to control them, we thus slightly modified the function governing the pulse interactions among the oscillators, with the goal to introduce contracting dynamics. Thus we can manipulate the properties of the unstable attractors through the cooperation of expanding and contracting dynamics.

We then study the local dynamics with both expanding and contracting dynamics. We derive evolution rate of phase difference between two active firing oscillators. When the rate becomes less than one, the local dynamics of the original unstable attractor actually becomes contracting. Thus the original unstable attractor is controlled to be a stable attractor. The controlled basin size is directly related to the width of the modified interval. Besides, we show that such controlled attractors are useful in generating switching dynamics that is only sensitive to large perturbations, and is insensitive to smaller perturbations falling within the small basins. Thus this approach can be used to process information with switching dynamics where noises or disturbances are unavoidable.

Here the presented method can only control unstable attractors with certain types of symbolic events. How all unstable attractors with various event structures can be controlled is still an open question. Similar to the method here, we need to consider the state of active firing oscillators at the arrival of pulses from themselves, as these oscillators are the source of unstable local dynamics. Furthermore, we need to study the effect of the split of a large number of simultaneously active firing oscillators, which means that the unstable local dynamics occurs in a high dimensional phase space.

References

[1] Edward O 2002 *Chaos in Dynamical Systems* (2nd Edn.) (Cambridge: Cambridge University Press)
[2] Zhang G T and Wang F Q 2018 *Chin. Phys. B* **27** 018201
[3] Dudkowski D, Jafari S, Kapitaniak T, Kuznetsov N V, Leonov G A and Prasad A 2016 *Physics Reports* **637** 1
[4] Bao J H and Chen D D 2017 *Chin. Phys. B* **26** 080201
[5] Tang Y X, Khalaf A J M and Rajagopal 2018 *Chin. Phys. B* **27** 040502
[6] Wang Y, Zheng G C and Liu C X 2018 *Acta Physica Sinica* **67** 050502
[7] Schittler Neves F and Timme M 2012 *Phys. Rev. Lett.* **109** 018701
[8] Timme M, Wolf F and Geisel T 2002 *Phys. Rev. Lett.* **89** 154105
[9] Timme M, Wolf F and Geisel T 2003 *Chaos* **13** 377
[10] Ashwin P and Timme M 2005 *Nonlinearity* **18** 2035
[11] Milnor J 1985 *Commun. Math. Phys.* **99** 177
[12] Broer H, Efstathiou K and Subramanian E 2008 *Nonlinearity* **21** 1385
[13] Zou H L, Deng Z C, Hu W P, Aihara K and Lai Y C 2017 *Nonlinear Dyn.* **89** 887
[14] Mirollo R E and Strogatz S H 1990 *SIAM J. Appl. Math.* **50** 1645
[15] Tsodyks M, Mitkov I and Sompolinsky H 1993 *Phys. Rev. Lett.* **71** 1280
[16] Vreeswijk C V 1996 *Phys. Rev. E* **54** 5522
[17] Gerstner W 1996 *Phys. Rev. Lett.* **76** 1755
[18] Kanamaru T and Aihara K 2010 *Neural Comp.* **22** 1383
[19] Luccioli S and Politi A 2010 *Phys. Rev. Lett.* **105** 158104
[20] Zou H, Gong X and Lai C H 2010 *Phys. Rev. E* **82** 046209
[21] Zou H L, Li M, Lai C H and Lai Y C 2012 *Phys. Rev. E* **86** 066214
[22] Kirst C and Timme M 2008 *Phys. Rev. E* **78** 065201(R)
[23] Schittler Neves F and Timme M 2009 *J. Phys. A: Math. Theo.* **42** 345103
[24] Zou H L, Katori Y, Deng Z C, Aihara K and Lai Y C 2015 *Chaos* **25** 103109
[25] Hartle H and Wackerbauer R 2017 *Phys. Rev. E* **96** 032223
[26] Ashwin P, Creaser J and Tsanevaatanasova K 2018 *arXiv* 1804.00550